The new Ensemble of Data Assimilations

LARS ISAKSEN, JAN HASELER,
ROBERTO BUIZZA, MARTIN LEUTBECHER

AN ENSEMBLE of Data Assimilations (EDA) system will be introduced at ECMWF with cycle 36r2 of the Integrated Forecasting System (IFS). The EDA system consists of an ensemble of ten independent lower-resolution 4D-Var assimilations that differ by perturbing observations, sea-surface temperature fields and model physics. The computing cost is significant, similar to running the deterministic analysis suite.

The main justification for implementing the EDA is that it quantifies analysis uncertainty.

- It is the first system implemented at ECMWF that provides estimates of analysis uncertainty. A properly designed EDA will complement the data assimilation system with important information about the quality of the deterministic analysis.
- It can be used to estimate flow-dependent background errors in the deterministic 4D-Var assimilation system; this will potentially improve the medium-range forecast. Flow-dependent background errors will be introduced in the second phase, in the autumn of 2010.
- It can improve the representation of initial uncertainties for the Ensemble Prediction System (EPS). When the EDA is introduced in IFS cycle 36r2, EDA-based perturbations will replace evolved singular vectors (SVs) to generate the EPS initial conditions. This change will improve the EPS skill, especially over the tropics.

The application of EDA in EPS will be described in an accompanying article by *Buizza et al.* in this issue of the *ECMWF Newsletter* (pages 22 to 28).

The EDA is expected to become an important part of the ECMWF data assimilation system, with the introduction of a hybrid 4D-Var/EDA system. Also, in the coming years, the EPS and EDA are expected to be further integrated to the benefit of both systems.

Rationale for developing an EDA system

The EDA is based on a perturbed lower-resolution version of the operational analysis system. If the perturbations of observations and model physics are realistic, the EDA will provide good estimates of analysis uncertainty. Because four-dimensional data assimilation, similar to that used for the operational analysis, is an integral part of EDA it has the potential to provide very valuable information about analysis uncertainty of the operational assimilation system. This is difficult to obtain by other means. The system will also provide short-range forecast error uncertainty. Many applications would benefit from accurate estimates of the uncertainty in analysis and short-range forecast errors. This could provide guidance for the quality of ECMWF's short-range forecasts. The EDA can also be used to improve the data assimilation system and the EPS.

In data assimilation, one of the crucial aspects is the estimation of the background error variances. To a large degree these are static in the operational 4D-Var system. This is unrealistic, especially for extreme events, where the background error variances can be underestimated significantly.

The EDA system is able to produce flow-dependent estimates of analysis uncertainty and background error uncertainty based on the ensemble spread, measured as the standard deviation of the difference between independent short-range background forecasts (*Fisher*, 2003; *Tan et al.*, 2007). This information gives an estimate of the error-of-the-day and can also be used for the estimation of seasonally varying background errors. Recent research at ECMWF has shown a beneficial impact from using the EDA errors of the day in the operational high-resolution 4D-Var. This is expected to be implemented in the second half of 2010.

Currently, covariance statistics of background error are generated from an offline EDA that is run over a period of one month. Only rarely are the statistics updated, and a single set of statistics is used for all seasons. The availability of an operational EDA will allow more frequent updates of background error statistics, with the possibility of accounting for seasonal variation of error covariances.

Characteristics of the EDA system

4D-Var at ECMWF is based on the incremental approach to minimising a cost function. The first minimisation (inner loop) takes place at low resolution to produce preliminary low-resolution analysis increments with a simplified representation of linearized model physics. The subsequent loops are at higher resolution with a more advanced linearized model physics applied. The comparison of observations against model fields takes place at a high resolution with all the non-linear aspects included (outer loop). This incremental approach provides considerable flexibility in the use of computer resources.

Isaksen et al. (2007) describe the design of the EDA in detail, based on analyses run with a T255 outer loop and T95/T159 inner loops and 91 vertical levels. In the EDA, for each observation, perturbations are defined by randomly sampling a Gaussian distribution with zero mean and standard deviation equal to the estimate of the observation error standard deviation. For cloud-track wind observations, perturbations are horizontally correlated. Sea-surface temperature fields are also perturbed, with correlated patterns as currently used in the Seasonal Forecasting System. At the first assimilation cycle, the randomly-perturbed observations are the only source of difference between the perturbed analyses, while for the subsequent cycles differences will evolve in the first-guess fields and contribute to the analyses spread. Model error is simulated by stochastically perturbing the model tendencies using same method applied in the EPS –

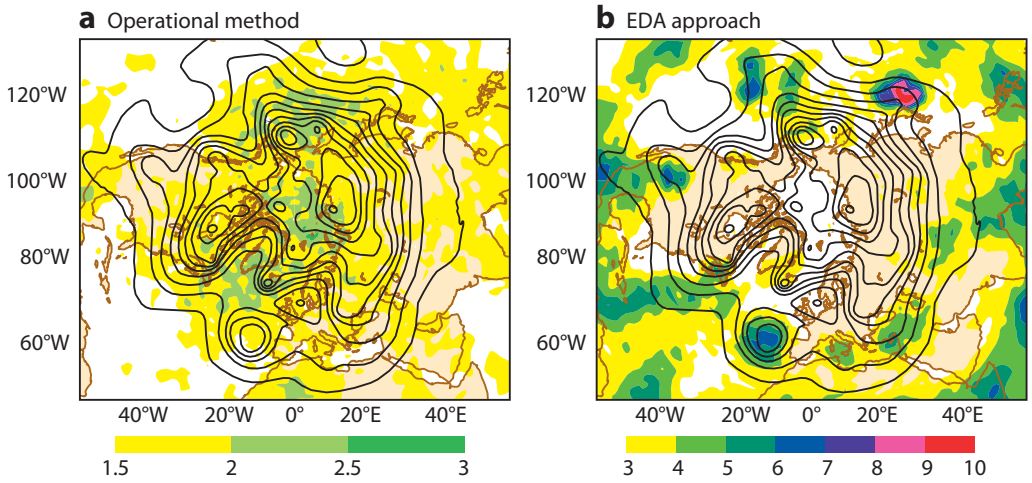

Figure 1 Background error standard deviation estimates for 850 hPa zonal wind at 00 UTC on 16 October 2006 using (a) the operational randomization method of *Fisher & Courtier*, 1995 (maximum value 2.97 ms^{-1}) and (b) the EDA approach based on 2 times the standard deviation of 10 ensemble members using T255 outer loop and T95/T159 inner loop (maximum value 9.99 ms^{-1}). Both panels have 500 hPa geopotential height field overlaid (8 dm contouring). The factor of two makes the average global EDA spread more realistic.

the method used is described later in the section on '*The operational EDA configuration*'.

Isaksen et al. (2007) demonstrated the EDA system's ability to produce flow-dependent spread and deliver promising results for some extreme meteorological events. The EDA produces a realistic horizontal distribution of analysis error and background error, with small values over the data rich areas of the USA, Europe and Australia.

Figure 1 shows a snapshot of background error estimates for 850 hPa zonal wind on a day in October 2006 for the northern hemisphere extra-tropical region from the operational randomization method (*Fisher & Courtier*, 1995) and the standard deviation of a ten member EDA. The EDA values have been scaled to get more realistic global average amplitude of variances. It is clear that the day-to-day background error estimates for wind have very different structures and amplitudes for the operational method (Figure 1a) and the EDA (Figure 1b). The operational method takes some account of flow curvature, but primarily samples the static background error variances, taking account of the observation coverage.

It is seen from Figure 1 that the EDA method results in more flow-dependent variability of the background error variances. The largest values are seen east of Japan where an extra-tropical low is developing. The EDA method really captures the dynamically active regions, like extra-tropical lows and troughs; an ability that to a large extent is lacking for the operational method.

The impact of EDA resolution and ensemble size has been investigated for the case used in Figure 1. Some results are now described that focus on the region near Japan that is dynamically very active. For the low-resolution assimilation system with one T95 inner loop (Figure 2c) there is a clear flow dependence, but this is not the case when the operational randomization method is used (Figure 2a). Also, the low-resolution assimilation system (Figure 2c) delivers less focussed, but still similar results compared to a higher-resolution system with two (T95 and T159) inner loops (Figure 2b). Both use a T255 outer-loop resolution.

Comparing Figures 2c and 2d, one can see the impact of increasing the number of ensemble members from 10 to 50. The patterns are very similar, but the result of the 50-member ensemble is smoother with fewer spikes and also reduces regions with very low variance. The 50 members are basically giving a statistically better sampling of the forecast errors, but they also describe flow-dependent features at a higher resolution. The results shown in Figure 2 suggest that computer resources may be better spent on more members with a simpler low-resolution version of the 4D-Var system. But more research investigating case studies of extreme events will have to be performed before the final conclusions can be drawn on this subject.

The capturing of flow dependence for all three ensemble-based versions shown in Figure 2 is clearly visible. The smoothing property of using 50 members is also marked. Indeed, the amplitudes and structures are surprisingly similar for the low- and higher-resolution analysis system. This may well be due to the fact that all systems for these experiments used a T255 outer-loop resolution. It is at this stage and resolution that the observations are perturbed. The uncertainty information is also propagated in time with the same T255 model resolution.

The EDA is most beneficial for extreme events. As an example, consider the Category-3 Hurricane Emily on 20 July 2005 just before it made landfall in Mexico. Figure 3a shows the precipitation measured by the local weather radar. The EDA spread (i.e., the standard deviation of the ten, in this case T399 members) for zonal wind at approximately 850 hPa is given in Figure 3b. Typical standard deviations in the region would be 2–3 ms^{-1}, but the flow-dependent estimates from the EDA system yield standard deviations up to 13 ms^{-1}. Note that the spread is concentrated in the vicinity of Hurricane Emily, identified by the mean sea level pressure contours.

The ability of the EDA system to identify regions of large background error associated with extreme events has the potential to significantly improve quality control decisions and give higher weight to observations used in the analysis from such regions.

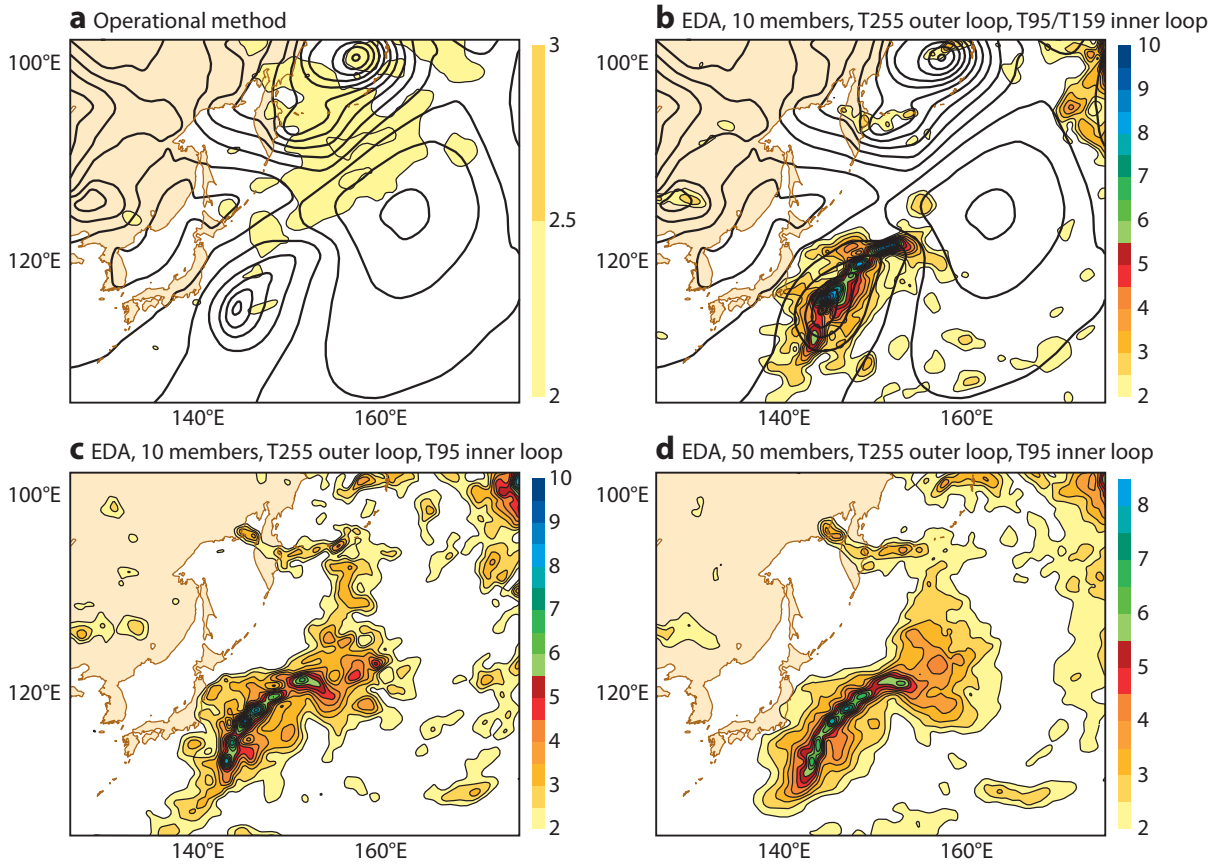

Figure 2 850 hPa zonal wind background error estimates valid at 00 UTC on 16 October 2006 for a baroclinic area near Japan. (a) The operational cycling randomization method (global max. 2.8 ms^{-1}). (b) The 10-member T255 outer loop with T95/T159 inner loop (global max. 13.8 ms^{-1}). (c) The 10-member T255 outer loop with T95 inner loop (global max. 13.9 ms^{-1}). (d) The 50-member T255 outer loop with T95 inner loop (global max. 12.0 ms^{-1}). Panels (b), (c) and (d) all use 2 times standard deviation of the ensemble members. The factor of two makes the average global EDA spread more realistic.

Deciding the operational configuration

It is important to note that the EDA system is designed to serve the needs of applications in the data assimilation system and the needs of the EPS. This has major implications for the design of the Ensemble of Data Assimilations that will become operational.

To be able to use the system to calculate background error statistics and estimate flow-dependent background errors, the EDA system must be designed to be sufficiently similar to the operational 4D-Var assimilation system. So it requires the same number of vertical levels (91 at present). The horizontal resolution cannot be significantly lower than the operational 4D-Var resolution in order to get a flow-dependent impact on extreme events and analysis uncertainty estimates that describe the operational 4D-Var system. Also, for reasons of consistency, a 4D-Var configuration in the EDA is preferable to a 3D-Var configuration.

When EDA products are used to calculate initial uncertainties for the EPS it will require vertical interpolation from 91 to 62 levels and horizontal interpolation from T399 to T639. It has been decided not to force the EPS and the EDA resolutions to be the same. This leaves more flexibility in the future system design of EPS and EDA. If the resolution of the EDA becomes an issue for the EPS the situation needs to be revisited. However, the computer codes have been designed to cater for any resolution change, as this may be required for research experiments or future operational configurations.

The performance and computing costs of a number of potentially suitable low-resolution configurations were investigated to choose an assimilation system that was close in skill to the operational system, but still significantly cheaper. The investigations described above, performed at T255, showed that a 10 member EDA system gave similar ensemble spread patterns to a 50-member EDA system, though with more noise. Because noise-filtering methods are available it was decided to choose 10 members for the initial operational implementation.

It was also seen that a higher-resolution outer loop was the main contributor to increased, more detailed ensemble spread and more accurate analysis uncertainty estimates. For the same inner-loop resolution, it was found that an increase in outer-loop resolution from T255 to T399 also improves the forecast scores significantly. The investigations showed that a T95 inner loop is not capable of representing tropical cyclones and other extreme events accurately. On the other hand, the use of a T255 inner loop added significant extra computing costs without a significant gain in EDA variance estimates.

It turned out to be more beneficial to increase the outer-loop resolution combined with use of a moderate inner-loop resolution. It should be kept in mind that because the EDA

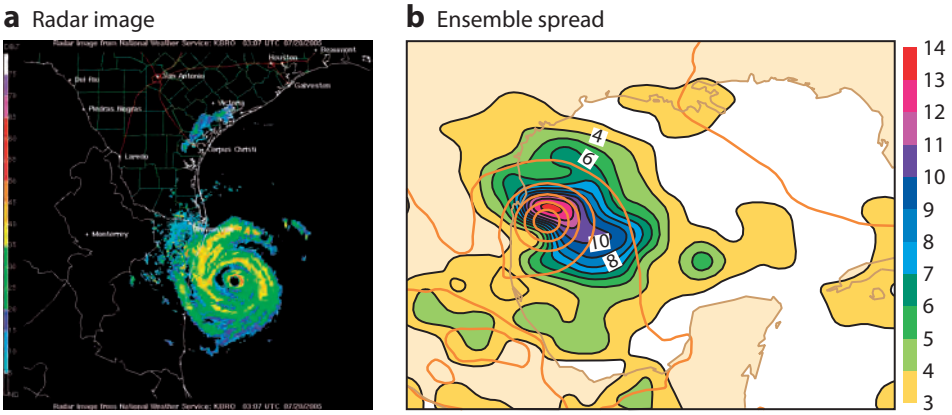

Figure 3 Atlantic hurricane Emily on 20 July 2005 near the coast of Mexico. (a) Radar image from National Weather Service. (b) Ensemble spread for zonal wind at 850 hPa near Hurricane Emily; the maximum value is 13.4 ms^{-1}. The mean sea level pressure contours are overlaid.

system only produces 15-hour forecasts (not 10-day forecasts) the cost of increasing the outer loop and forecast resolution from T255 to T399 is relatively small.

The operational EDA configuration

Based on these investigations it was decided to use the following configuration for the operational EDA system.

- The EDA system is run at T399L91 resolution with a control (unperturbed) analysis and 10 perturbed analyses.
- The analyses are 12-hour 4D-Var, with two minimizations, first at T95, then at T159 with advanced linearized physics.
- The EDA is run twice daily, with the midnight analyses using observations from 2101 UTC to 0900 UTC and the midday analyses using observations from 0901 UTC to 1500 UTC.
- The observations used are those which have already been extracted for the operational high-resolution delayed cut-off 12-hour 4D-Var analysis, so the EDA analyses can run as soon as these observations become available.
- Unperturbed observations are used for the control analysis, while the other members use observations which have been modified by a random perturbation which is proportional to the observation error.
- For Atmospheric Motion Vector (AMV) observations, the perturbations are horizontally correlated.
- Input sea surface temperature fields are perturbed using the same method as for the seasonal forecasts.

In the EDA it is important to represent model error to account for the fact that the forecast model is not perfect. To simulate the impact of model uncertainty, the stochastically perturbed parametrization tendency (SPPT) scheme is used; this perturbs the total parametrized tendency of physical processes. Positive results have also been obtained with the stochastic backscatter (SPBS) scheme that is based on the idea of backscatter of kinetic energy from unresolved scales (see *Palmer et al.*, 2009 for a review of ECMWF work on stochastic parametrization schemes). To date, however, the use of the SPPT scheme alone gave the best performance (work is in progress to assess the impact of also introducing a backscatter scheme).

On average, if the EDA spread is measured in terms of the 700 (850) hPa temperature standard deviation, the SPPT scheme increases the global average by 19% (23%), and if the EDA spread is measured in terms of the 700 (850) hPa the kinetic energy standard deviation is increased by 33% (39%).

It is interesting to see the geographical distribution of model error impact on short-range forecast uncertainty implied by the stochastic methods. Figure 4 shows the zonally averaged EDA spread for temperature (Figure 4a) and zonal wind (Figure 4b) valid on 14 October 2008 when SPPT is used. The impact of SPPT on the spread can be assessed by calculating the ratio of EDA spread from an experiment with SPPT applied compared to EDA spread from an experiment without model error parametrization. It is clear that the increase in spread due to SPPT is significant for both temperature (Figure 4c) and zonal wind (Figure 4d) throughout the atmosphere. The largest SPPT impact for temperature is at the top of the planetary boundary layer, especially in the stratocumulus regions. For wind the largest impact is near 700 hPa in the tropics. The SPBS only perturbs the wind field directly, so the increased spread in temperature (Figure 4e) is small. The increased wind spread for the SPBS scheme (Figure 4f) is mainly located in the planetary boundary layer, where the convection is most active. It is clear that the SPPT scheme provides more widespread perturbations than the SPBS. The larger level of spread looks reasonable and gives the best improvement of the EPS system.

Figure 4 confirms that the SPBS and SPPT methods complement each other, but the new tendency stochastic physics is the more effective of the two methods. Further testing will be performed with both methods applied. This is linked to the medium term goal of unifying the model error representations in the EPS and EDA.

Future developments

A well-designed EDA system will enable improved estimates of analysis uncertainty. This will be a potentially valuable output from the Centre's data assimilation system.

For the EDA, the short-term improvements will take account of horizontal correlations for radiance observation errors, use OSTIA instead of NOAA/NESDIS sea-surface temperatures (as already is the case in the operational 4D-Var), and improve the perturbations applied to the surface observations and parameters. Further investigations will be performed to assess the benefit of more ensemble members, various model error representations and different assimilation configurations. Finally, a significant effort is ongoing to develop and implement the use of flow-dependent background error in the deterministic 4D-Var system.

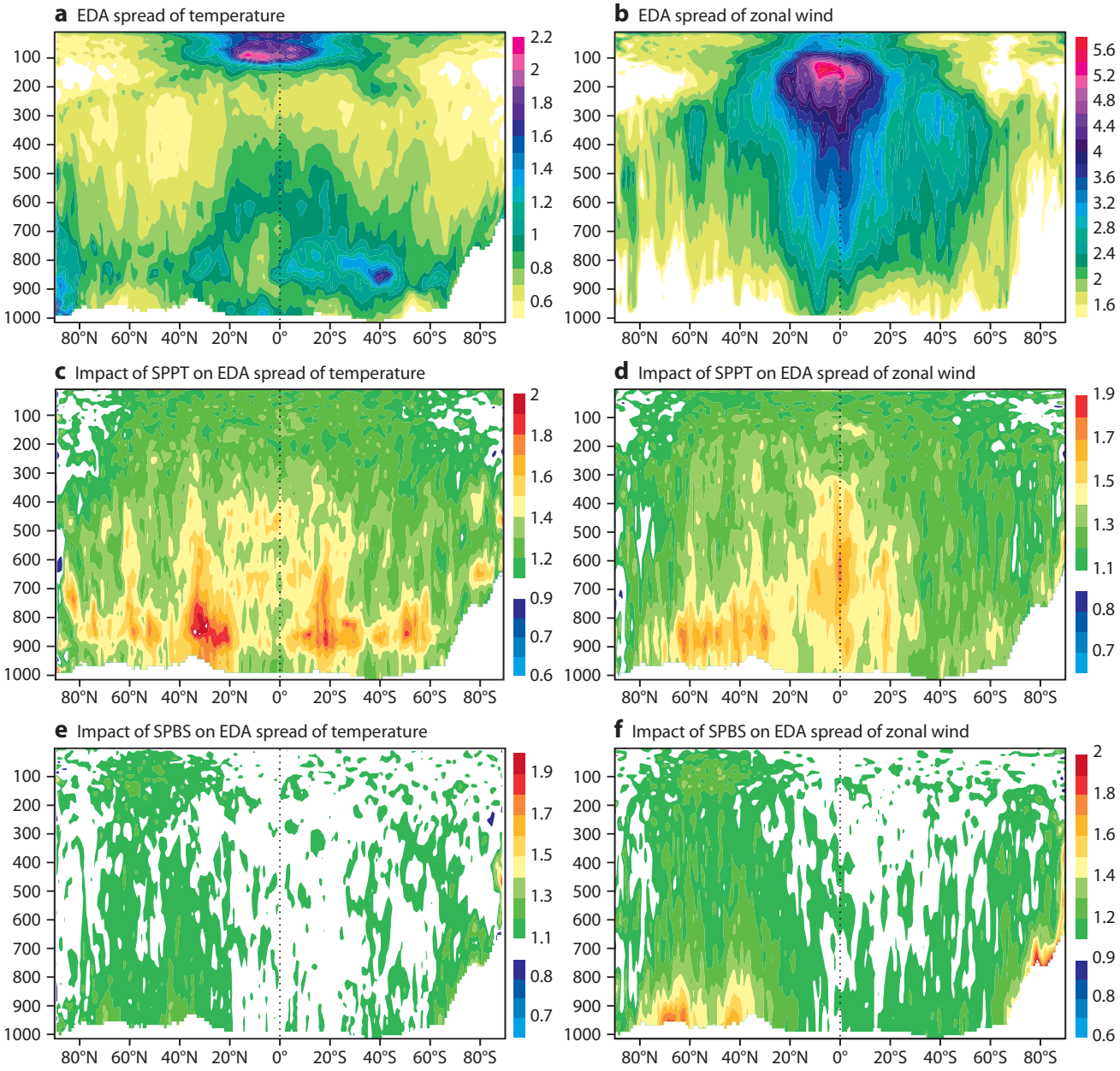

Figure 4 Impact of model error representation on EDA spread. Zonal mean values for (a) temperature and (b) zonal wind on 14 October 2008 using the operational SPPT configuration. The ratio of EDA spread for SPPT applied compared to EDA spread without model error parametrization for (c) temperature and (d) zonal wind. The same ratios for (e) temperature and (f) zonal wind when SPBS is used. As expected, the ratios are almost always greater than one.

FURTHER READING

Buizza, R., M. Leutbecher, L. Isaksen & J. Haseler, 2010: The use of EDA perturbations in the EPS. *ECMWF Newsletter No. 123*, 22–28.

Fisher, M., 2003: Background error covariance modelling. In Proc. *ECMWF Seminar on Recent developments in data assimilation for atmosphere and ocean,* 8–12 September 2003, 45–63. http://www.ecmwf.int/publications/library/do/references/list/17111

Fisher, M. & P. Courtier, 1995: Estimating the covariance matrices of analysis and forecast error in variational data assimilation, *ECMWF Tech. Memo. No. 220.* http://www.ecmwf.int/publications/library/do/references/list/14

Isaksen, L., M. Fisher & J. Berner, 2007: Use of analysis ensembles in estimating flow-dependent background error variance. In *Proc. ECMWF Workshop on Flow-dependent Aspects of Data Assimilation*, 11–13 June 2007, 65–86. http://www.ecmwf.int/publications/library/do/references/list/14092007

Palmer, T.N., R. Buizza, F. Doblas-Reyes, T. Jung, M. Leutbecher, G.J. Shutts, M. Steinheimer & A. Weisheimer, 2009: Stochastic parametrization and model uncertainty. *ECMWF Tech. Memo. No. 598.* http://www.ecmwf.int/publications/library/do/references/list/14

Tan, D.G.H., E. Andersson, M. Fisher & L. Isaksen, 2007: Observing system impact assessment using a data assimilation ensemble technique: application to the ADM-Aeolus wind profiling mission. *Q. J. R. Meteorol. Soc.*, **133**, 381–390.

Combined use of EDA- and SV-based perturbations in the EPS

ROBERTO BUIZZA, MARTIN LEUTBECHER, LARS ISAKSEN, JAN HASELER

THE SIMULATION of initial uncertainties is one of the key aspects in ensemble prediction. At ECMWF, since the implementation of the first version of the Ensemble Prediction System (EPS) in 1992, these uncertainties have been simulated with singular vectors (SVs), perturbations characterized by the fastest growth, measured using a total energy norm, over a finite time interval.

With the forthcoming implementation in cycle 36r2 of an Ensemble of Data Assimilations (EDA, see the companion article in this edition of the *ECMWF Newsletter*, pages 17 to 21), the methodology used to generate the EPS initial perturbations will be changed. EDA-based perturbations will replace evolved singular vectors in the generation of the EPS initial conditions. Following this change, the EPS initial perturbations will have a better geographical and vertical coverage than in the earlier system. This results in a better spread-skill relationship in the early forecast range over the extra-tropics, and for the whole forecast range over the tropics. Limited-area ensemble prediction systems (e.g. COSMO-LEPS) that use EPS initial and boundary conditions will benefit from this improvement. Over the tropics the substantial increase of the EPS spread leads to much smaller spread under-dispersion. In terms of skill, the EDA-SVINI configuration of the EPS has a higher skill than the earlier SV-based system everywhere.

This article briefly describes the new EDA-SVINI implementation and discusses some results.

The old SV-based EPS

In the old SV-based system (Figure 1a), the EPS initial perturbations are generated using SVs growing over two different time periods:

- Evolved SVs (EVO) growing optimally during the 48 hours leading to the analysis time represent uncertainties that are likely to contribute most to analysis errors.
- Initial-time SVs optimally growing during the first 48 hours of the forecast (SVINI) sample directions in phase space likely to contribute most to forecast uncertainty.

Practically, the SVs are computed separately over the northern and the southern hemisphere extra-tropics, and for up to six local regions in the tropics to improve the geographical sampling of the initial uncertainties. The initial-time and evolved SVs for the different areas are re-scaled to have initial amplitude comparable to the analysis error estimate given by the high-resolution data-assimilation system. The background research that lead to ECMWF's SV-approach to simulating initial uncertainty is briefly summarized in Box A, and more detailed information about the configuration used to compute the SV component is given in Box B.

Replacement of the evolved SVs with EDA-based perturbations in the EPS

Buizza et al. (2008), who discuss in details the rationale behind the proposed change, have shown that replacing the

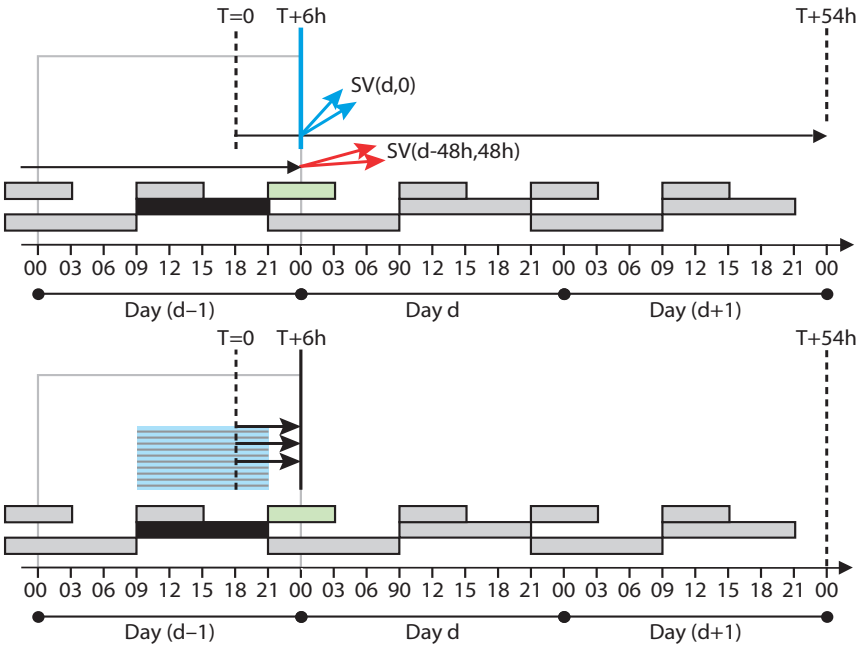

Figure 1 (from *Buizza et al.*, 2008). Schematic of the configuration used to generate the EPS initial conditions at 00 UTC. (a) The 12-hour-long black and grey boxes mark the time window of the 12-hour 4D-Var; while the 6-hour-long dark-grey and grey boxes for 21–03 UTC and 09–15 UTC mark the time window of the early-delivery 6-hour 4D-Var. The EPS unperturbed analysis at 00 UTC is defined by the 6-hour 4D-Var analysis generated by the early-delivery suite (green box). The evolved *SV(d-48h,48h)* (red vectors) are computed from 00 UTC of day *(d-2)*, and the initial-time *SV(d,0)* (blue vectors) are computed from 00 UTC of day d. The trajectory along which the *SV(d,0)* grow starts from the +6-hour forecast initiated at 18 UTC of day *(d-1)*, and the trajectory along which *SV(d-48h,48h)* grows starts from the +6-hour forecast initiated at 18 UTC of day *(d-3)*. (b) The EDA members used at day *d* (blue box with black lines) are generated by 12-hour 4D-Var cycles running between 09 UTC and 21 UTC of day *(d-1)*.

ECMWF's SV-approach to simulating initial uncertainty

A

The ECMWF SV-approach to simulating initial uncertainty using SVs was inspired by earlier work by, among others, *Lorenz* (1965) and *Farrell* (1990), who showed that these type of perturbations dominates the system dynamics over a finite time-interval. It is worth also quoting the work of *Ehrendorfer & Tribbia* (1997), who showed that if the objective of an ensemble system is the optimal prediction of the forecast error covariance matrix (optimal in the sense of maximum possible fraction of forecast error variance), then the singular vectors constructed using covariance information at the initial time constitute the most efficient means for predicting the forecast error covariance matrix. *Palmer et al.* (1998) discussed the issue of the impact of the norm definition on the SVs, and argued that the total energy norm used in the ECMWF system is a good approximation of the covariance matrix mentioned by Ehrendorfer & Tribbia.

evolved SVs with EDA-based initial perturbations leads to a better ensemble system. In the new EDA-SVINI configuration (Figure 1b):

- EDA-based perturbations are used instead of the evolved SVs to represent uncertainties that have been growing during the data assimilation cycles.
- Initial-time SVs optimally growing during the first 48 hours of the forecast (SVINI) were used to sample directions likely in phase space to contribute most to forecast uncertainty.

The EDA perturbed members are generated by (a) perturbing all observations and the sea-surface temperature field and (b) using the stochastically perturbed parametrization tendency (SPPT) scheme that perturbs the total parametrized tendency of physical processes to simulate random model error. More details on the EDA methodology can be found in the companion article by *Isaksen et al.* published in this edition of the *ECMWF Newsletter*,

In this new EDA-SVINI configuration, the EPS initial conditions are defined by adding to the unperturbed analysis an EDA-based perturbation and a linear combination of initial-time SVs. The initial-time SV component is identical to the one that was used in the old EVO-SVINI configuration except for a reduction of the amplitude by 10%. This reduction of the SVINI component is needed to achieve a better spread-skill relationship since the EDA-based perturbations have larger amplitude than the EVO component.

Each EDA-based initial perturbation is defined by the difference between one perturbed and the un-perturbed 6-hour forecasts (the first-guess) started from the previous EDA cycle (i.e. from the EDA 4D-Var analyses run during the 12-hour period preceding the most recent analysis used to generate the unperturbed analysis). The EDA-based perturbations are symmetric, thus the EPS initial perturbations are still symmetric in the new configuration.

The reason why differences between 6-hour first guesses from the preceding EDA assimilation cycle are used instead of differences between analyses, is that the EDA suite runs with a 12-hour delayed mode to achieve a timely dissemination of the EPS products. Earlier experimentation compared ensemble forecasts using EDA-based perturbations defined by analyses and perturbations defined by 6-hour forecasts from the preceding cycle. Published (*Buizza et al.*, 2008) and recent results indicated that the use of 6-hour forecast perturbations instead of analyses perturbations does not degrade the probabilistic skill of the EPS. It should be pointed out that the EDA-based perturbations are also added to the upper-level specific humidity component of the unperturbed initial conditions (this variable was not perturbed in the old EVO-SVINI configuration). The reader is referred to *Buizza et al.* (2008) for a more detailed discussion of the similarity and differences between the old SV-based and the new EDA-based configurations.

Replacement of the evolved SVs with EDA-based perturbations in the EPS re-forecast suite

Since March 2008, when the 15-day variable resolution ensemble was merged with the monthly prediction system, a key component of the EPS system has been the EPS re-forecast suite (*Hagedorn*, 2008; *Hagedorn et al.*, 2010). The EPS re-forecast suite is based on a 5-member ensemble starting from ERA-Interim analyses, and run for the same calendar day of the past 18 years. These 90 forecasts are used operationally to generate monthly anomaly products

The old EVO-SVINI configurations of the EPS

B

In the old EVO-SVINI configuration, the initial conditions are defined by adding to the unperturbed analysis a linear combination of initial-time and evolved SVs. To optimize the use of computational resources, SVs for any specific day/time are computed along a forecast trajectory, defined by the 6-to-54 hour forecast starting from a 6-hour earlier analysis (see *Leutbecher*, 2005 for more information).

For the EPS starting at time *t*, the initial-time SVs are the initial-time (*t*=0) SVs computed along a 6-to-54 hour forecast starting at *t*= –6 h. The evolved SVs are the final-time (*t*+48 h) SVs computed along a 6-to-54 h forecast starting at *t*= –54 h. The initial perturbations are symmetric, with the EPS even members having the opposite sign perturbation of the odd members. The coefficients that determined the linear combination and the amplitude of the SVs are computed using a Gaussian sampling method.

Over the extra-tropics (northern and southern hemispheres) the 50 leading initial-time and extra-tropical SVs are used, and over the tropics only the 5 leading initial-time SVs for each tropical target area are used (see *Leutbecher & Palmer*, 2008 for details). These perturbations are added only to the temperature and wind component of the model state vector, and to the surface pressure (no perturbations are added to the specific humidity or to any surface field). In the new EDA-SVINI configuration of the EPS only the initial-time SVs are used.

Initial conditions			EPS forecasts day 0–15/32	
Unperturbed analysis	SV-based initial perturbations	EDA-based initial perturbations	Leg A (day 0–10)	Leg B (day 10–15/32)
T639L62 (interpolated from T1279L91 operational analysis)	T42L62	T399L62 analyses interpolated from the T399L91 analyses	T639L62	T319L62

Table 1 Resolution of the components used to generate the EPS initial conditions and produce the EPS forecasts since 26 January 2010.

and to compute EPS products such as the Extreme Forecast Index (to be more precise, the EFI uses 450 forecasts, i.e. the 90 re-forecasts starting on the 5 weeks centred on the current day).

The new EDA-SVINI configuration will be used also for the re-forecast suite, but since the EDA has not been run for the past years, the re-forecast suite has to use the EDA-based perturbations computed for the current year. More precisely, since the re-forecasts are run up to 2-weeks in advance, the re-forecasts for any specific day for the past 18 years use the EDA-based perturbations from the current year minus 14 days. Extensive experimentation has indicated that the EDA-SVINI re-forecast EPS, despite using EDA perturbations from another year, has spread and skill characteristics closer to the real-time EPS than the old EVO-SVINI re-forecast EPS (not shown).

Comparison of the old EVO-SVINI and the new EDA-SVINI EPS configurations

It is worth noting that since 26 January 2010, the EPS has been running with a T639L62 (spectral triangular truncation at wave-number 639 with a linear grid and 62 vertical levels) resolution between day 0 and 10, and with T319L62 resolution from day 10 to day 15 (day 32 at 00 on Thursdays) – this is referred to as the 639v319 EPS. Table 1 summarizes the resolution of the key components of the EDA-SVINI configuration of the EPS that will become operational with model cycle 36r2 (the re-forecast suite has the same characteristics, but it includes only 4 instead of 50 perturbed members).

EPS initial perturbations

The replacement of the evolved SVs with EDA-based perturbations has a large impact on the EPS initial perturbations As an example, Figure 2 shows the initial perturbations in terms of temperature and the zonal wind component at 700 hPa for one randomly-chosen member, member number 5, of the EVO-SVINI (left panels) and the EDA-SVINI (right panels) ensembles started on 1 December 2009. Also Figure 3 shows the corresponding results for a vertical cross section. The EDA-SVINI perturbations are less localized geographically and in the vertical and provide a better coverage of the globe. This is true especially over the tropics which were sampled (by design) only in a limited fashion by the initial perturbations of the old EVO-SVINI system.

The EDA-based perturbations, computed at T399 resolution, have smaller scales than T42 SV-based perturbations

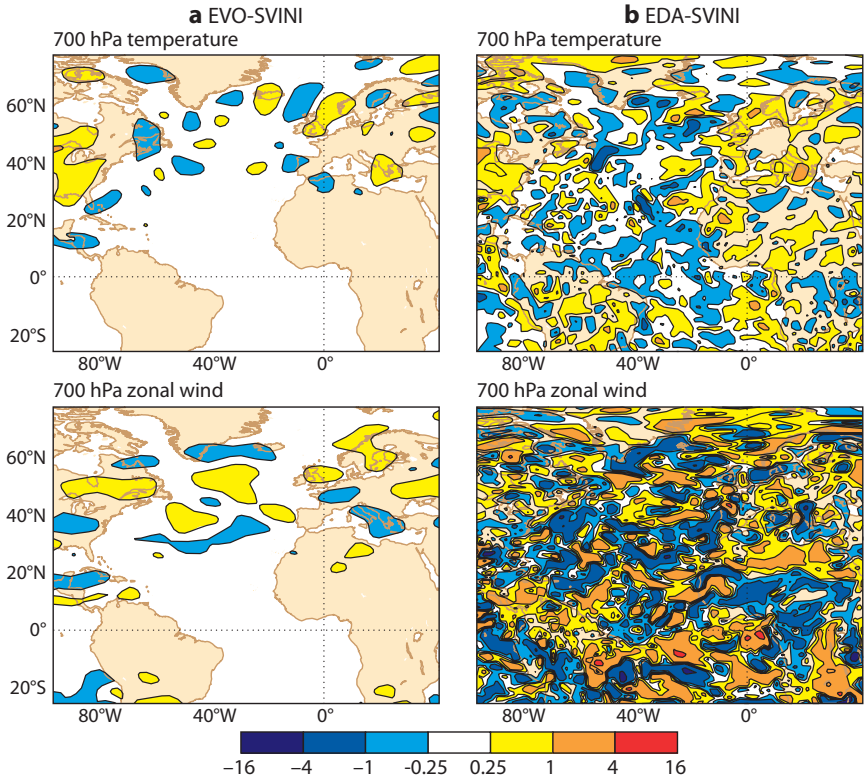

Figure 2 Initial-time perturbation of EPS member number 5 of (a) EVO-SVINI and (b) EDA-SVINI started at 12 UTC on 1 December 2009, in terms of the 700 hPa temperature (top panels) and the 700 hPa zonal wind (bottom panels).

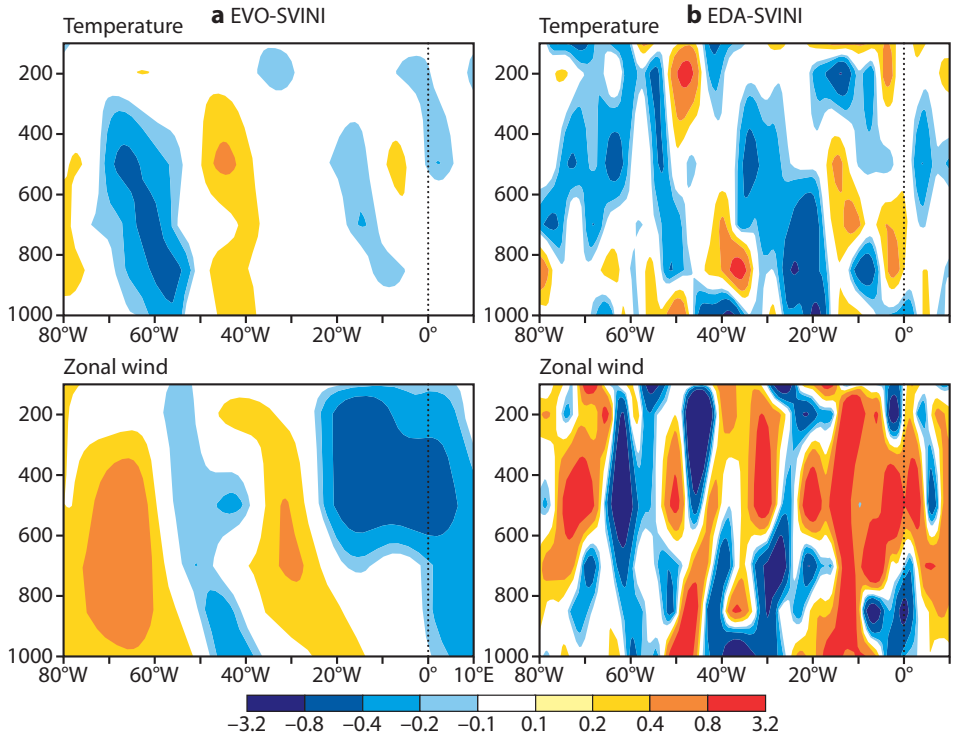

Figure 3 As Figure 2 but for a vertical cross section at latitude 50°N between 80°W and 10°E of the perturbation of EPS member number 5 of (a) EVO-SVINI and (b) EDA-SVINI at 12 UTC on 1 December 2009, in terms of temperature (top panels) and zonal wind (bottom panels).

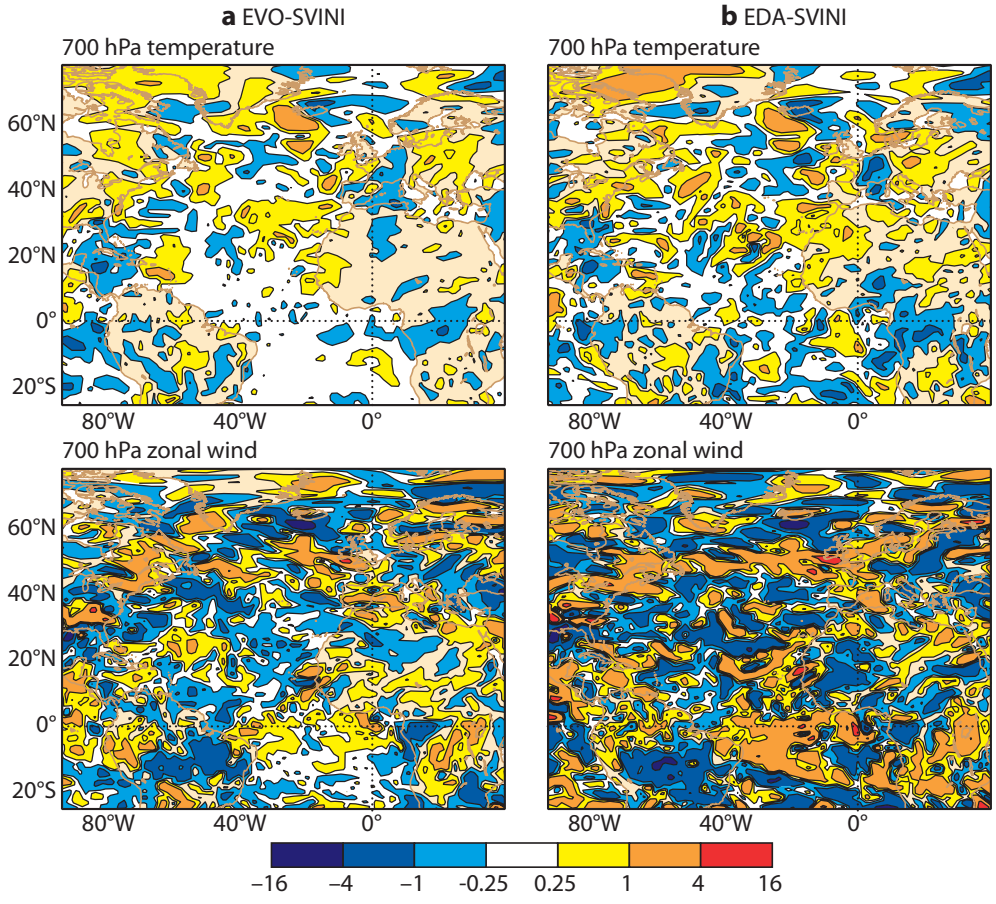

Figure 4 As Figure 2 but for the t+24 hour perturbation of EPS member number 5 of (a) EVO-SVINI and (b) EDA-SVINI started at 12 UTC on 1 December 2009, in terms of the 700 hPa temperature (top panels) and the 700 hPa zonal wind (bottom panels).

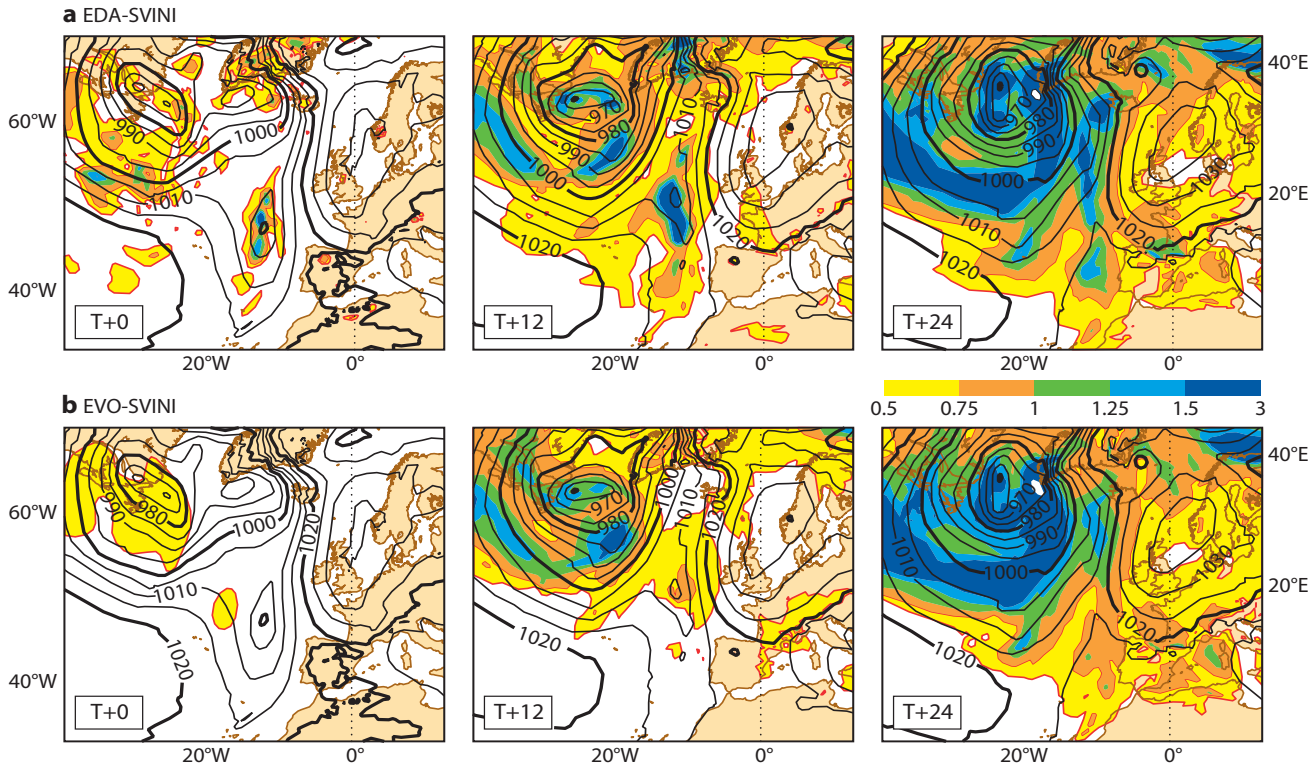

Figure 5 Ensemble-mean (black contours) and standard deviation (coloured shading) in terms of mean-sea-level-pressure (MSLP) of (a, top panels) EDA-SVINI and (b, bottom panels) EVO-SVINI ensembles at initial time (left panels), at T+12 hour (middle panels) and at T+24 hour (right panels) for EPS forecasts started on 11 December 2009. The contour interval for the ensemble-mean fields is 5 hPa; the shading for the standard deviation is for 0.5, 0.75, 1.0, 1.25, 1.50 and 3 hPa.

and a less evident vertical tilt with height. In addition, the EDA-based perturbations grow slower than SV-based perturbations, which explains why an ensemble with only EDA-based initial perturbations would have too little spread and a poorer performance than an EDA-SVINI ensemble (see *Buizza et al.*, 2008). By contrast, the blend of EDA-based perturbations and the initial-time SVs combines the benefits of both sets of diverse perturbations, and provides a superior performance to EVO-SVINI.

The effect of the modified initial perturbations is detectable over the extra-tropics during the first 48 hours and over the tropics for the first week. The EDA-SVINI perturbations start with a larger initial amplitude than the EVO-SVINI perturbations but after 24 hours their amplitude is close to the amplitude of the EVO-SVINI perturbations, especially over the extra-tropical regions where the SVINI component starts dominating the perturbation growth (Figure 4). This is the reason why from this forecast time on, in the regions sampled by initial-time SVs, the perturbations from the two ensembles have similar structures (e.g. south-east of Greenland (20°W, 60°N) or south-east of Cuba (60°W, 10°N)). But in the regions not sampled by the initial-time SVs (e.g. over most of the tropics) the EDA-SVINI initial perturbations provide a better geographical coverage. After 48 hours, over the extra-tropics the difference becomes, on average, smaller and gradually disappears in the medium-range (say around forecast day 7).

Member States' users of EPS initial and boundary conditions for limited area ensemble prediction systems over Europe will benefit from the increased spread over the extra-tropics in the early forecast range. This can be seen in Figure 5; this example shows the ensemble spread at initial time and at T+12 and T+24 hours for the EPS started at 12 UTC on 11 December 2009. The EDA-SVINI has a larger initial spread at 20°W where the EDA perturbed analyses differ slightly in the positioning and intensification of a low-pressure system, which propagates in time and leads to larger spread at T+24 hours west of Spain.

EPS spread and skill characteristics

The difference in the characteristics (amplitude, scale, growth rate, coverage) of the initial-time perturbations affects the average ensemble spread, as can be seen in Figure 6. This shows the 10-day average (forecasts with initial date from 1 to 19 December 2009, every other day) spread of the EVO-SVINI and the EDA-SVINI ensembles in terms of the 850 hPa temperature and the 700 hPa kinetic energy. The EVO-SVINI initial perturbations (left panels) are much more localized and have a smaller amplitude than the EDA-SVINI initial perturbations (right panels).

Figure 7 shows the average impact on 639v319 ensemble forecasts of the 850 hPa temperature, based on the comparison of EVO-SVINI and EDA-SVINI initial perturbations for 88 cases (from 5 October to 31 December 2009). As already mentioned in the introduction, in the EDA-SVINI ensemble, the amplitude of the SVINI perturbations has been decreased by 10% to improve the spread and skill relationship.

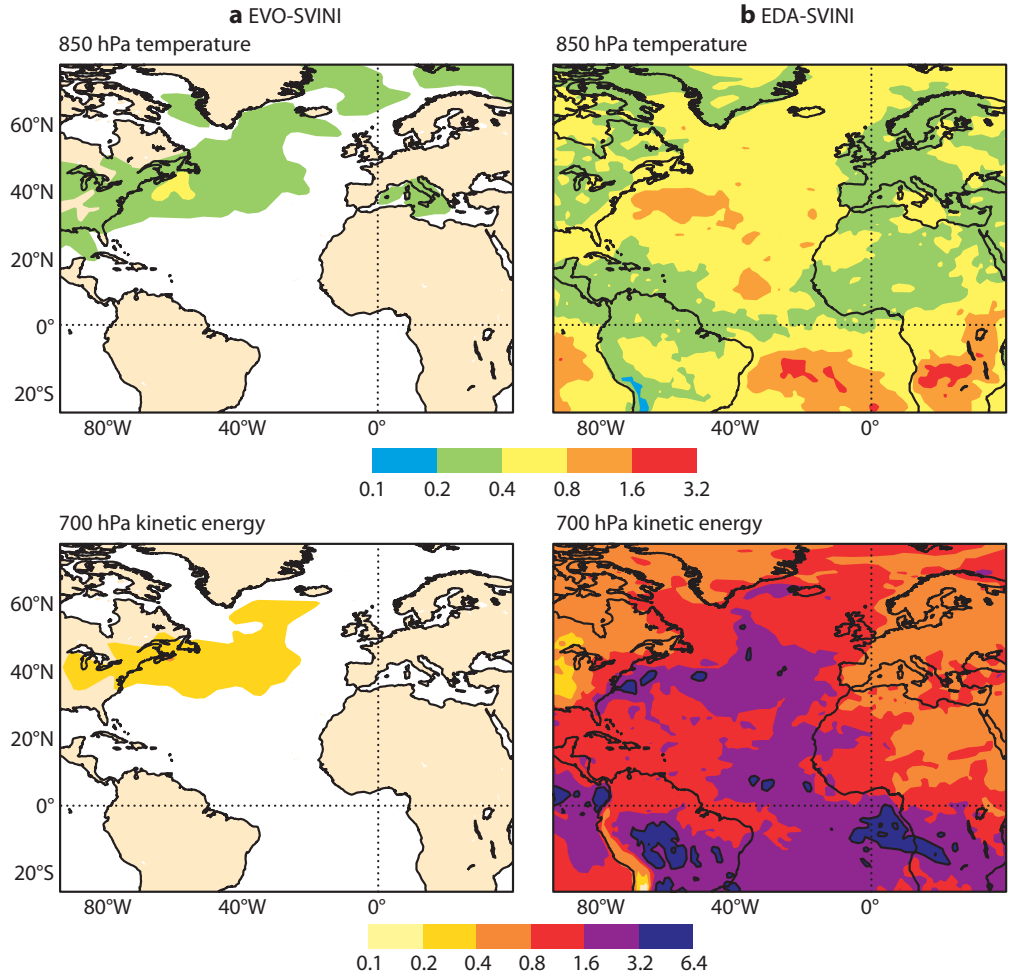

Figure 6 Ensemble spread: 10-case average (1 to 19 December 2009, every 2 days) standard deviation at initial time of an (a) EVO-SVINI ensemble and (b) EDA-SVINI ensemble, measured in terms of the 850 hPa temperature (top panels, K) and the 700 hPa kinetic energy (lower panels, ms^{-1}).

The EDA-SVINI ensemble has, on average, a better-tuned ensemble spread and a higher skill. Over the extra-tropics, there is a clear increase in ensemble spread during the first 48 hours: this reduces the spread under-estimation of the old ensemble system by about 50%. There is also a small positive impact on the error of the ensemble-mean and on the skill of probabilistic scores measured by the continuous rank probability skill score (CRPSS): although small, differences are statistically significant at the 5% level up to forecast day 6 over the northern hemisphere, and up to forecast day 10 over the southern hemisphere.

The positive impact on the ensemble spread and skill is more evident over the tropics, where the use of the EDA-based perturbations has a large impact on the ensemble spread. Over this region, the EDA-SVINI ensemble-mean has a smaller root-mean-square-error that is statistically significant (at the 5% level) and the probabilistic forecast has a higher continuous ranked probability skill score up to forecast day 9.

Similar conclusions can be drawn from other probabilistic accuracy measures, such as the area under the relative operating characteristic curve or the Brier skill score (not shown).

Future developments of the EPS

Work will continue in four key areas to further improve the skill of the EPS:

- ***EDA membership***: the potential benefit of using a larger ensemble of perturbed analyses (25 or 50 instead of 10) will be assessed.
- ***EDA-based land-surface perturbations***: spread of the EPS in the boundary layer and for surface variables will be assessed more thoroughly, and the potential use of EDA-based perturbations to perturb surface variables (e.g. soil moisture and soil temperature) will be investigated.
- ***Combination of EDA- and SV-based perturbations***: possible ways to combine the EDA- and the SV-based perturbations different from the one implemented in the EPS will be explored, with the final aim to provide a better tuned and more skilful ensemble system for the entire forecast range and for the whole vertical structure of the atmosphere.
- ***Stochastic model error***: revised and new stochastic schemes are under final development and will be tested in the EPS and the EDA to improve the simulation of model uncertainties.

Progress in these areas will be reported in due course.

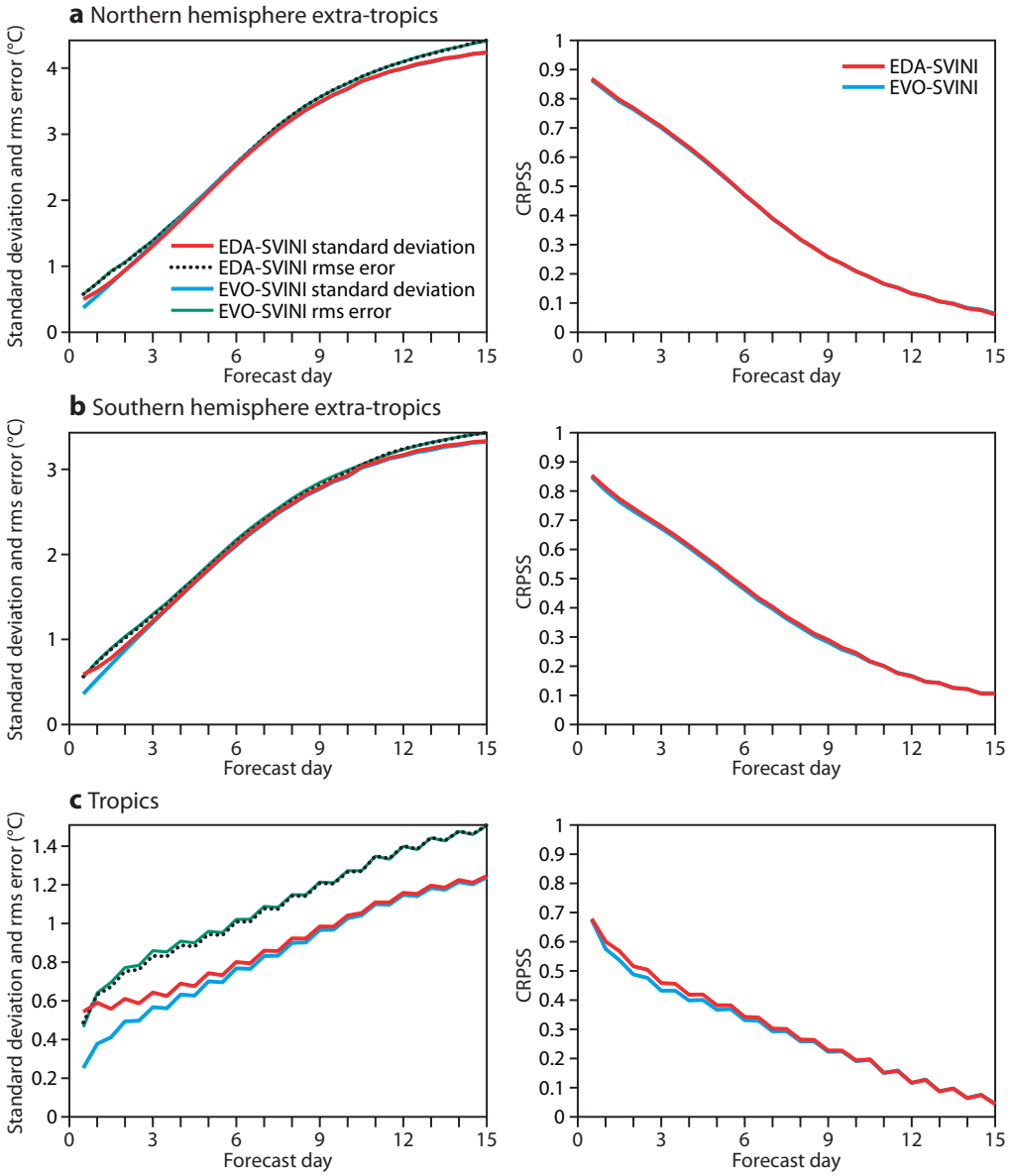

Figure 7 Average (88 cases from 5 October to 31 December 2009) statistics for the 850 hPa temperature over (a) northern hemisphere extra-tropics, (b) southern hemisphere extra-tropics, and (c) tropics. Left: root-mean-square error of the ensemble-mean forecast of the EDA-SVINI and the EVO-SVINI ensembles, and standard deviation of the EDA-SVINI and the EVO-SVINI line) ensembles. Right: continuous rank probability skill score (CRPSS) of the EDA-SVINI and the EVO-SVINI ensembles.

FURTHER READING

Buizza, R., M. Leutbecher & L. Isaksen, 2008: Potential use of an ensemble of analyses in the ECMWF Ensemble Prediction System. *Q. J. R. Meteorol. Soc.*, **134**, 2051–2066.

Ehrendorfer, M. & J.J. Tribbia, 1997: Optimal prediction of forecast error covariances through singular vectors. *J. Atmos. Sci.*, **54**, 286–313.

Farrell, B.F., 1990: Small error dynamics and the predictability of atmospheric flows. *J. Atmos. Sci.*, **47**, 2409–2416.

Hagedorn, R., 2008: Using the ECMWF re-forecast dataset to calibrate EPS forecasts. *ECMWF Newsletter No. 117*, 8–13.

Hagedorn, R., R. Buizza, M.T. Hamill, M. Leutbecher & T.N. Palmer, 2010: Comparing TIGGE multi-model forecasts with re-forecast calibrated ECMWF ensemble forecasts. *Mon. Wea. Rev.*, submitted.

Isaksen, L., J. Haseler, R. Buizza & M. Leutbecher, 2010: The new Ensemble of Data Assimilations. *ECMWF Newsletter No. 123*, 17–21.

Leutbecher, M., 2005: On ensemble prediction using singular vectors started from forecasts. *Mon. Wea. Rev.*, **133**, 3038–3046.

Leutbecher, M. & T.N. Palmer, 2008: Ensemble forecasting. *J. Comp. Phys.*, **227**, 3515–3539.

Lorenz, E., 1964: A study of the predictability of a 28-variable atmospheric model. *Tellus*, **17**, 321–333.

Palmer, T.N., R. Gelaro, J. Barkmeijer & R. Buizza, 1998: Singular vectors, metrics, and adaptive observations. *J. Atmos. Sci.*, **55**, 633–653.